# COLOR SEPARATION FOR 7-INK PRINTING USING FM SCREENING

Mei-Chun Lo*, Jui-Chang Chiang+, Lester Shi♣

Keyword:characterization, component, gamut, KCR, masking, neugebauer

**Abstract**: The purpose of 7-ink CMYKRGB printing, with FM screening, is to extend the color gamut beyond what can be achieved in the conventional 4-ink process. Due to the addition and proportionality failure of inks, the characterization of the 7-ink printing process is more complex than the characterization of 4-ink printing process. The approach carried out in this study lowers the complexity of the characterization problems by subdividing the 7 inks into 6 subsets of 4-ink grouping. Each subset comprises 3 chromatic inks and black ink. The masking-type (2nd) and the Neugebauer-type (Cellular Neugebauer) algorithms, based on the use of colorimetric transformations from ink to color, were derived to model the 6 subsets of 4-ink grouping. The results showed that the 2nd model performed better than the Cellular Neugebauer model. Additionally, the separate test target is required for the characterization of neutral and near-neutral colors to further improve the accuracy of predictions for the models derived. It was also found that the highly saturated colors having less gray contents provide the severe test to the derived models' performance.

## INTRODUCTION

The colors reproduced in multi-color printing tend to become darker provided

*Dept. of Graphic Communication and Technology, The World College of Journalism and Communications <lo@gc.wcjc.edu.tw>
+Shen's Art Printing Co.<raymond @shen.com.tw>
♣Institute of Paper-Making and Graphic Arts, Chinese Culture University <lester@shen.com.tw>

that more inks are used due to the subtractive interaction of inks and the incident light. The purer and more colorful colors of red, green and blue are difficult to be reproduced using the traditional set of CMYK primary inks, since they have to be produced by overlapping two inks of CMY primaries. However, more optimal or desired colors of Red, Green, and Blue can be obtained using the single Red, Green and Blue inks respectively instead of using 2-ink overprints of the CMY primaries. Furthermore, the gamut of printable colors can be extended by augmenting a set of CMYK inks with additional inks. The expansion of regions include darker tone, and especially the quarter and three quarter tones. The Frequency-Modulated (FM) (Humbel et al. 1992) screening, an technique promising an end to the moire problem, makes this job easily to be implemented.

## Subdivision Approach and Modeling Color Behavior for 7-ink Printing Process

The purpose of this study was to use 7-ink CMYKRGB printing process, with FM screening, to extend the color gamut beyond what can be achieved in the conventional 4-ink printing process. The approach carried out is based on the scheme suggested by Harold Boll (1993). The 7 inks, CMYKRGB, were grouped into 6 subsets of 4-ink grouping (see Table 1). These 6 subsets are KRYG, GKYC, KGCB, BKMC, KBMR, and RKYM. Each subset consists of 3 chromatic inks and black ink. These 6 subsets of 4-ink groupings represent 6 adjacent and overlapping subgamuts of the 7-ink CMYKRGB supergamut in color space (as shown in Figure 1). Each subgamut reproduced using the corresponding inkset was individually characterized as a conventional CMYK color gamut. The device characterization here is defined as the provision of data for developing a mathematical transformation which determines the conversion between device-dependent data and device-independent colorimetric data based on the CIE system. Thus, the characterization of 7-ink printing process in this study is modeling method developed by measuring a number of colors produced using each subset of 4-ink grouping to define the transformation separately.

Table 1. The category of 4-ink grouping

| Dominant Component (ink) | Subgamut | Key Component (ink) |
|---|---|---|
| Yellow | KRYG | Black (K) |
| Green | GKYC | Green (G) |
| Cyan | KGCB | Black (K) |
| Blue | BKMC | Blue (B) |
| Magenta | KBMR | Black (K) |
| Red | RKYM | Red (R) |

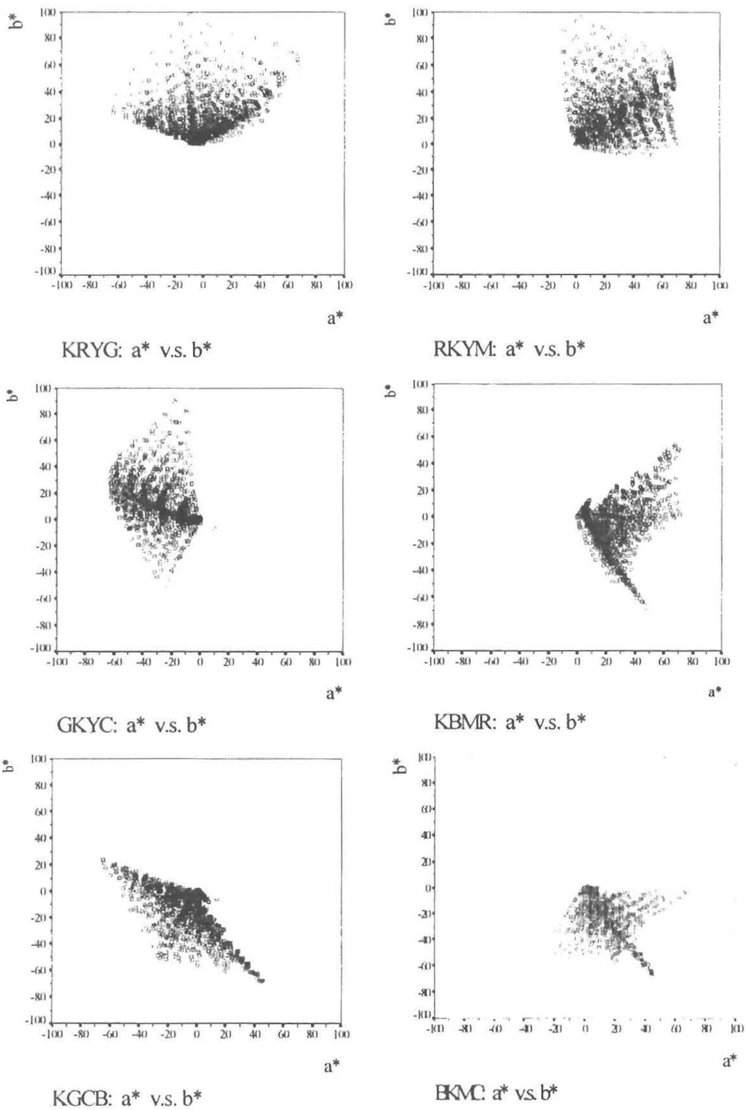


Figure 1. View of 6 subsets of 4-ink grouping including KRYG, GKYC, KGCB, BKMC, KBMR, and RKYM in CIELAB color space

A colorimetric equivalency is present between the CMY and black inks in the traditional CMYK printing process. The typical term-GCR (Gray Component Replacement) refers to the removal of the third contaminant color (i.e. gray component) produced from a combination of three primary colors, CMY,and its replacement with black instead. Similarly, a term-KCR (Key Component Replacement) was used in this paper. It refers, e.g. in KRYG subgamut, to reduce or remove a key component-black (i.e. gray) made up of paired inks R and G, and replace it with a corresponding amount of black ink. As listed in Table 1, the key component in the subgamuts of KGCB and KBMR is black as the subgamut of KRYG. The black ink in the subsets of KRYG, KGCB, and KBMR is thus called key ink. As for subgamuts of GKYC, BKMC, and RKYM, the key components are green, blue and red respectively. Theoretically, using KCR (for instance in the subset of GKYC), the key component green, made up of paired inks yellow and cyan, could be reduced and replaced with an equivalent amount of green ink.

## Review of Mathematical Models For Characterizing Printing Devices

One fundamental question for a color reproduction system in Graphic Arts (Pobboravsky and Pearson 1972) is:

*"What is the mathematical relationship between how a color looks and the amounts of printing colorants required to produce a visual match?".*

This is the question concerned with the form of a mathematical transformation to correlate between the output primary signals generated and the input required. In practical application, an optimal reproduction of a color image is needed to transform between the device-dependent, and device-independent coordinates, thereby the appearance of any colors can be colorimetrically specified.

Basically, printing mathematical models can be mainly divided into two types of equations: Neugebauer-type and Masking-type. Each mathematical model includes two forms: a forward and a reverse. The forward process calculates the CIE tristimulus values from a set of printing device primaries, for instance, CMY or CMYK for conventional printing devices; or RYG or KRYG for one of subgamuts used in this research. The reverse process predicts a set of primaries from a corresponding set of tristimulus values. The section below introduces some mathematical models, including the Neugebauer-type and the Masking-type, applied for characterizing 7-color imaging device in this research.

### Neugebauer-type Equations

The Neugebauer-type model (1937) is a theoretical approach in relation to the ink amounts of the color considered when a color is produced by halftone process. It predicts the colors which result from small halftone dots using data from large solid areas or 100% fractional dot areas (FDAs), known as Neugebauer Primaries. The Algorithm is essentially an additive color model, based on the additive color theory and the assumption that the halftone dots are randomly distributed on the print. The resultant color appearance on a print seen by an observer is due to the fusion of the reproduction primaries (Cyan, Magenta, Yellow, Red, Green, Blue, White, Black for three-color CMY reproduction) in the eye. In other words, the tristimulus values of the reproduction color pixel can simply be obtained by summing the tristimulus values of the combination of Neugebauer primaries, and weighting each by the relative fractional dot area.

The basic Neugebauer model computes the FDAs related to the halftone (tint) dot areas of the single-colored CMY on paper, using the Murray-Davies equations (Murray 1936).

If the XYZ tristimulus values of the eight Neugebauer primaries in a three color reproduction system are represented as below:

| Color | Tristimulus Values |
|---|---|
| White | $X_{PW}$, $Y_{PW}$, $Z_{PW}$ |
| Cyan | $X_{CS}$, $Y_{CS}$, $Z_{CS}$ |
| Magenta | $X_{MS}$, $Y_{MS}$, $Z_{MS}$ |
| Yellow | $X_{YS}$, $Y_{YS}$, $Z_{YS}$ |
| Red | $X_{RS}$, $Y_{RS}$, $Z_{RS}$ |
| Green | $X_{GS}$, $Y_{GS}$, $Z_{GS}$ |
| Blue | $X_{BS}$, $Y_{BS}$, $Z_{BS}$ |
| 3-color (Overprint) | $X_{3CS}$, $Y_{3CS}$, $Z_{3CS}$ |

the basic Neugebauer-type model can be expressed as Eqn. 1.

$$
\begin{aligned}
X &= f_p X_{PW} + f_c X_{CS} + f_m X_{MS} + f_y X_{YS} + f_r X_{RS} + f_g X_{GS} + f_b X_{BS} + f_{3c} X_{3CS} \\
Y &= f_p Y_{PW} + f_c Y_{CS} + f_m Y_{MS} + f_y Y_{YS} + f_r Y_{RS} + f_g Y_{GS} + f_b Y_{BS} + f_{3c} Y_{3CS} \\
Z &= f_p Z_{PW} + f_c Z_{CS} + f_m Z_{MS} + f_y Z_{YS} + f_r Z_{RS} + f_g Z_{GS} + f_b Z_{BS} + f_{3c} Z_{3CS} \qquad (1)
\end{aligned}
$$

where

- X, Y, Z are the tristimulus values of the color resultant or to be matched.
- fi value is the fractional dot area (FDA) of the paper covered by the indicated primary (the value ranging between 0.0 and 1.0).
- subscripts p, c, m, y, r, g, b, 3c refer to the Paper White, Cyan, Magenta, Yellow, Red (i.e. Magenta + Yellow), Green (i.e. Cyan + Yellow), Blue (i.e. Cyan + Magenta) reproduction primaries (tints) respectively.

However there are a number of problems limiting the accuracy of the basic Neugebauer model. The major problem arises from the scattering of light within paper because the reflection does not occur at the ink-paper interface. This effect needs to be correctly predicted for an accurate color reproduction. Although the Murray-Davies equation does take this into account, it cannot predict this effect accurately.

Yule and Nielsen (1951), Clapper and Yule (1955), and Yule and Colt (1961) suggested that more accurate predictions could be made if the Neugebauer equation was modified to include an appropriate power factor (known as $n$ value) to account for the internal reflections and scattering within the paper. With a power law, the basic Neugebauer model discussed above was modified to include an exponent ($1/n$) for the tristimulus values in both sides of equation. This is known as the Yule-Nelson modified Neugebauer model. With the addition of a Black primary (K), the number of possible overlaps is 16 rather than 8. The previous Neugebauer equations can be further extended to include the original eight primaries and the overprinting of the black primary.

The previous two Neugebauer-type models introduced were limited to use only a set of 8 samples or 16 samples for three- or four- colour cases respectively. Heuberger et al. (1992) found that the Neugebauer-type models, with the addition of partial dot area coverages, could produce more accurate results than the original model. A more accurate modified Neugebauer model can be derived using more than eight sample prints in a three-colour reproduction. The addition of these partial overprint samples is equivalent to partitioning the CMY space into rectangular cells and expanding the Neugebauer-type equations within each cell. Hence, a set of dot areas c, m, y can be represented as a point in a three-colour CMY space. This type of model is referred to as the Cellular Neugebauer-Type Model.

The forward process of the Neugebauer-type models calculates the XYZ values directly from the dot area values (FDAs) of primary inks. The FDA values have to be calculated by a numerical method in the reverse process.

**Masking-Type Equations**

Another model used to correlate the printing primaries and the CIE XYZ system is the masking-type model. The technique used for deriving the forward and reverse processes in the Masking-type Models is the same. Therefore, only the forward models are introduced here.

The original first-order masking equations were devised by Yule (1938). It assumes the occurrence of additivity and proportionality of ink densities as the halftone dot area, or colorant concentration or film thickness changes. Thus a simple linear transformation would be sufficient to establish the amount of inks required in the reproduction in order to match the three color intensities in the original copy. In practice, serious departures from additivity and proportionality arise because of the halftone screen and turgidity of the media. Hence, Clapper (1961) suggested an expansion of the original masking equations with the inclusion of 2nd-order terms to give a more accurate prediction than that of the first-order model. Yule (1967) subsequently suggested that greater accuracy could be obtained by using higher order polynomials such as 2nd-order and 3rd-order. The forward 3rd-order masking models used in this research are given in Eqn. 2.

$$
\begin{aligned}
D_r = \; & a_1 c + a_2 m + a_3 y + a_4 c^2 + a_5 m^2 + \\
& a_6 y^2 + a_7 c m + a_8 c y + a_9 m y + a_{10} c^3 + \\
& a_{11} m^3 + a_{12} y^3 + a_{13} c^2 m + a_{14} c^2 y + a_{15} m^2 c + \\
& a_{16} m^2 y + a_{17} y^2 c + a_{18} y^2 m + a_{19} c m y \qquad (2)
\end{aligned}
$$

where

- similar terms are used for calculating $D_g$, $D_b$.
- $a_i$ represent the coefficients.
- c, m and y values (normalized into 0.0 to 1.0) are the principal colorimetric densities on paper which can be obtained by establishing a one-dimensional look-up-table (LUT) between the fractional dot areas on film (FDAs) and colorimetric densities on paper for each of three primaries.

The LUT is a technique whereby the relationship between two variables is specified as a table in which one group of variables is defined on one column of table, and the related group of variables listed in the other column. Therefore, the relationship between two variables can be linearly interpolated. The $a_i$, $b_i$ and $c_i$ coefficients can be optimized using a least-squares technique (e.g. derived by Lawson and Hanson (1972)) to give the closest colorimetric predictions to those measured. The $D_r$, $D_g$, $D_b$ and c, m, y are given by:

$$
\begin{aligned}
D_r &= \log ( X_o / X ) \\
D_g &= \log ( Y_o / Y ) \\
D_b &= \log ( Z_o / Z ) \qquad (3)
\end{aligned}
$$

$$
\begin{aligned}
c &= \log ( X_o / X_c ) \\
m &= \log ( Y_o / Y_m ) \\
y &= \log ( Z_o / Z_y ) \qquad (4)
\end{aligned}
$$

where

- ($D_r$, $D_g$, $D_b$) and (X, Y, Z) are the red-, green-, and blue- colorimetric densities and tristimulus values of a color stimulus respectively.
- $X_o$, $Y_o$ and $Z_o$ are the tristimulus values of the paper substrate (white).
- $X_c$, $Y_m$, $Z_y$ are the X value for the cyan, Y value for the magenta, and Z value for yellow tints (halftone) respectively.

In the following part of this paper, the $D_r$, $D_g$, $D_b$ are represented by $D_{r\text{-}3c}$, $D_{g\text{-}3c}$, $D_{b\text{-}3c}$, and $D_{r\text{-}4c}$, $D_{g\text{-}4c}$, $D_{b\text{-}4c}$ respectively for a three-color component and a reproduced (or original) four-color pixel respectively considered in one of 6 subgamuts. The c, m, y, for instant for KRYG subgamut, are substituted by $D_{r\text{-}R}$, $D_{g\text{-}Y}$, $D_{b\text{-}G}$ (called representative colorimetric densities in this study instead of principal colorimetric densities used by Lo et al. (1994)) for each of three single-colored tints of Red, Yellow, and Green Colorants respectively. The red-, green-, and blue- colorimetric densities of black ink are also calculated using Eqn. 3.

Lo et al. (1995) extended Johnson et al. (1995) and Luo et al. work (1992) to augment the three primaries CMY with black ink. Various BPA (Black printer Algorithm) models including Sub-Additivity Equations(SAE), Modified Sub-Additivity Equations (MSAE), Third-Order Polynomial Equations (3rd), and Second-Order Polynomial Equations (2nd), were derived and each consisted of both forward and reverse processes. The 2nd model was performed the best found in their results. In this study, the 2nd model was thus further extended and applied to characterize the 7-color printing process. The 2nd BPA model assumes that the three-color component and black component (i.e. key component) are two separate parts in CMYK four-color printing. Basically, this model is similar to the 2nd-order masking model in the three-color reproduction to apply all possible cross terms. In this case, 27 terms were used to include all possible combinations of $(D_r, D_g, D_b)_{4c}$ and $(D_r, D_g, D_b)_k$. The forward algorithm is given in Eqn. 5.

$$\begin{aligned}
D_{r\text{-}4c} = \; & a_{1,1} D_{r\text{-}3c} + a_{1,2} D_{g\text{-}3c} + a_{1,3} D_{b\text{-}3c} + \\
& a_{1,4} D_{r\text{-}k} + a_{1,5} D_{g\text{-}k} + a_{1,6} D_{b\text{-}k} + \\
& a_{1,7} D^2_{r\text{-}3c} + a_{1,8} D^2_{g\text{-}3c} + a_{1,9} D^2_{b\text{-}3c} + \\
& a_{1,10} D^2_{r\text{-}k} + a_{1,11} D^2_{g\text{-}k} + a_{1,12} D^2_{b\text{-}k} + \\
& a_{1,13} D_{r\text{-}3c} D_{g\text{-}3c} + a_{1,14} D_{r\text{-}3c} D_{b\text{-}3c} + a_{1,15} D_{r\text{-}3c} D_{r\text{-}k} + \\
& a_{1,16} D_{r\text{-}3c} D_{g\text{-}k} + a_{1,17} D_{r\text{-}3c} D_{b\text{-}k} + a_{1,18} D_{g\text{-}3c} D_{b\text{-}3c} + \\
& a_{1,19} D_{g\text{-}3c} D_{r\text{-}k} + a_{1,20} D_{g\text{-}3c} D_{g\text{-}k} + a_{1,21} D_{g\text{-}3c} D_{b\text{-}k} + \\
& a_{1,22} D_{b\text{-}3c} D_{r\text{-}k} + a_{1,23} D_{b\text{-}3c} D_{g\text{-}k} + a_{1,24} D_{b\text{-}3c} D_{b\text{-}k} + \\
& a_{1,25} D_{r\text{-}k} D_{g\text{-}k} + a_{1,26} D_{r\text{-}k} D_{b\text{-}k} + a_{1,27} D_{g\text{-}k} D_{b\text{-}k}
\end{aligned} \quad (5)$$

where

- similar terms are used for calculating $D_{g\text{-}4c}$, $D_{b\text{-}4c}$.
- $a_{i,j}$ are the optimized coefficients (i = 1 to 3 for $D_r$, $D_g$ and $D_b$ respectively) obtained by using the Lawson and Hanson least-squares technique to give the closest predictions to those the measured colorimetric data.
- ($D_{r\text{-}4c}$, $D_{g\text{-}4c}$, $D_{b\text{-}4c}$), ($D_{r\text{-}3c}$, $D_{g\text{-}3c}$, $D_{b\text{-}3c}$), ($D_{r\text{-}k}$, $D_{g\text{-}k}$, $D_{b\text{-}k}$) terms are the red-, green-, and blue- colorimetric densities of the four-color, three-color component, and key component respectively.
- The key components are black (K), Green (G), black (K), blue (B), black (K), and red (R) for subsets of KRYG, GKYC, KGCB, BKMC, KBMR, and RKYM respectively.

## EXPERIMENTAL

### Color Chart (Test Target)

The printing device selected was Screen Flat Bed Proofer. A printer characterization data set, i.e. a 6×6×6×6 matrix color chart was output for each subset of 4-ink grouping KRYG, GKYC, KGCB, BKMC, KBMR, and RKYM using an Imagesetter Aventra44 with FM screening, using the Agfa CristalRaster technique. It was then produced using the respective ink sets. Each subset was composed of 3 chromatic plus black inks as shown in Table 1. The samples in these data sets were squares of approximate 0.8 centimeter. Each color chart consists of 1296 patches, which represent all combinations of 4 inks varying in 6 values equally spaced over the fractional dot areas (FDAs) range of 0 to 100 with a 20 unit interval. In the KRYG color space (subgamut), for instant, each axis represents one of the four KRYG primaries and was divided into 6 divisions. In each subgamut, the first cube data set, produced using only three primaries without key primary ink (see Table 1) was used to derive the 3rd-order masking model. The overall samples in each subset were used to derive two characterization models for each corresponding subgamut. The component, referred to as dominant in each grouping, tends to be present to a greater degree than the other two chromatic components. Each 4-ink subset differs by only one ink from each of two adjacent subsets. This ensures that the entire superset of 6 color charts is a reasonable representation of all colors reproducible using 7 inks.

### Measurements

The spectral reflectance values of each sample, from the previously produced data sets, were obtained by using a Macbeth Color-Eye 3100 spectrophotometer. The measurements were performed at d/8 geometry of illuminating and viewing. Samples were taken over the range across the visible spectrum 360-740 nm with a 20 nm interval. Tristimulus values were calculated, against the real D50 light source of the viewing cabinet, using the method derived from Stearns (1975, 1985) abridged weights' method.

### Printing Characterization Models derived for 7-ink printing process

Two printing characterization models were derived and used to characterize each subset of 4-ink grouping. These were: the second-order polynomial model (designated as 2nd as described above) and the Cellular Neugebauer-type model.

Additionally, a third-order (3rd-order) masking model considering three-color components was included in the 2nd model derived. Only the computational procedure used in the 2nd model will be described using diagram below because it is more complicated than that used in the Cellular Neugebauer-Type model. As mentioned earlier, each subgamut reproduced using the corresponding inkset was individually characterized as a conventional CMYK color gamut. Figure 2 shows a schematic diagram for the computation of the forward 2nd model using the subset of KRYG as an

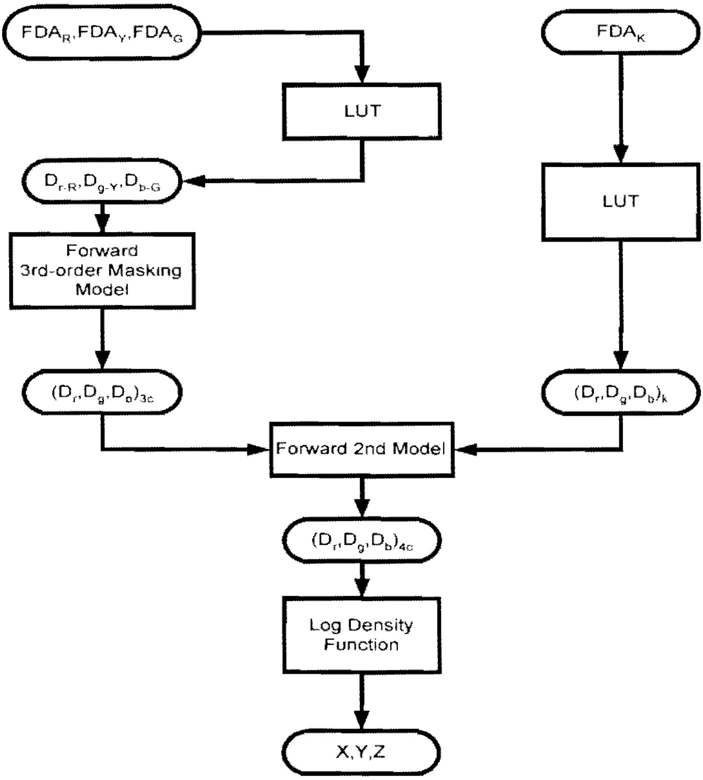


Figure 2 The Computational procedures used in the forward 2nd model for characterizing 7-ink printing process ( e.g in KRYG Subgamut )

example. The FDAs of KRYG inks are the input values. The FDAs of RYG are first converted to the representative colorimetric densities (i.e. $D_{r\text{-}R}$, $D_{g\text{-}Y}$, and $D_{b\text{-}G}$ respectively) via LUT, and the red-, green-, and blue- colorimetric densities of three-color component (i.e. $(D_r, D_g, D_b)_{3c}$) are then computed using the forward 3rd-order masking model. The FDA of K ink is used to obtain the red-, green-, and blue- colorimetric densities of the key component $(D_r, D_g, D_b)_k$ (i.e. black) via the LUT. Subsequently, a forward 2nd model is applied to predict the $(D_r, D_g, D_b)_{4c}$ of a resultant color by adding the key component $(D_r, D_g, D_b)_k$ to the three-color component $(D_r, D_g, D_b)_{3c}$ obtained in the earlier stage. Finally, the predicted tristimulus values (XYZ) are transformed from $(D_r, D_g, D_b)_{4c}$ using log density functions (Eqn. 3).

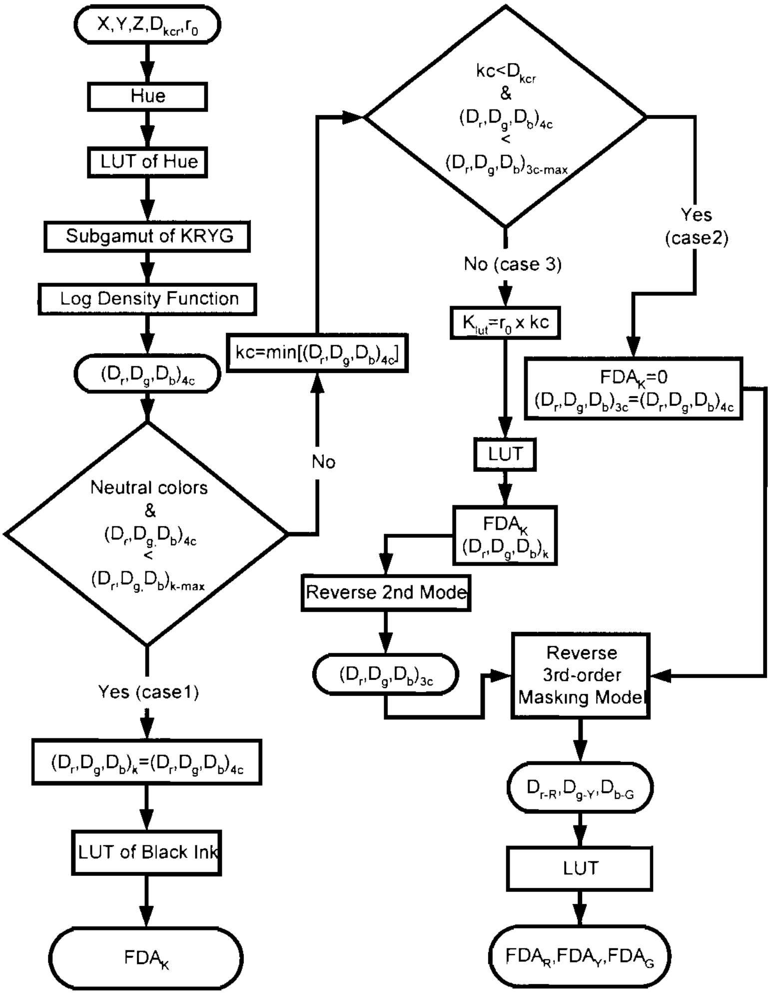


Figure 3. The Computational procedures used in the 2nd model complemented in supergamut CMYKRGB for characterizing 7-ink printing process (e.g. a target color predicted is produced using the subset of KRYG)

The reverse process includes a reverse 2nd model, and a reverse masking model. The reverse 2nd model can be considered as a key component replacement (KCR) algorithm as described earlier. Figure 3 illustrates the computational procedures of the full reverse 2nd model, applying key component replacement (KCR) in the supergamut CMYKRGB. Some parameters need to be defined as shown below.

| | |
|---|---|
| $D_{kcr}$ | critical density point below which no key component replacement is performed. This is predetermined, say $D_{kcr} = 0.6$. |
| $(D_r, D_g, D_b)_{3c\_max}$ | the red-, green-, and blue- colorimetric densities obtained from the sample produced using FDAs of 100% R, 100% G, and 100% B. |
| $(D_r, D_g, D_b)_{k\_max}$ | the red-, green-, and blue- colorimetric densities obtained from the sample produced using only key (black) ink with 100 % FDA. |
| kc | the key component defined by the smallest density of $(D_r, D_g, D_b)_{4c}$. |
| $r_0$ | the percentage of key component removed from each channel of $(D_r, D_g, D_b)_{4c}$ This is also predetermined. |
| $K_{lut}$ | the key component removed from the set of the input $(D_r, D_g, D_b)_{4c}$ and replaced by key (black) ink. |

In Figure 3, the XYZ values of a target color are first entered and then converted into CIE 1976 a, b hue angle, *hab*. The subset of 4-ink grouping, used for producing the target color, is then determined via LUT of Hue (through *hab*). The XYZ values are also transformed into $(D_r, D_g, D_b)_{4c}$ using the log density functions given in Eqn. 3. The next step is to predict the amount of key ink (K) used. Only the black content will be used if the color considered is neutral and its red-, green-, and blue- colorimetric densities ($(D_r, D_g, D_b)_{4c}$) are less than the respective channels of solid black ink (i.e. $(D_r, D_g, D_b)_{k\text{-}max}$ known previously). In this case (designated as Case 1), the $(D_r, D_g, D_b)_{4c}$ will be set to equal $(D_r, D_g, D_b)_k$, and the FDA of black used will be specified via LUT of black ink. Otherwise, Case 2 or 3 will be chosen. Case 2 excludes black ink (i.e. $FDA_k = 0$). This is determined by the smallest density of the $(D_r, D_g, D_b)_{4c}$ (i.e. kc less than $D_{kcr}$), and $(D_r, D_g, D_b)_{4c}$ less than $(D_r, D_g, D_b)_{3c\text{-}max}$. Hence the $(D_r, D_g, D_b)_{3c}$ are set equal to $(D_r, D_g, D_b)_{4c}$. In Case 3, the appropriate black content (i.e. $K_{lut}$) is calculated using the initially defined $r_0$, and followed by obtaining both the $FDA_k$ and $(D_r, D_g, D_b)_k$ via the LUT. Then, the $(D_r, D_g, D_b)_{3c}$ are obtained using a reverse 2nd model. Subsequently, the calculated $(D_r, D_g, D_b)_{3c}$ are used to obtain the representative colorimetric densities of the other three primaries (i.e. $D_{r\text{-}R}$, $D_{g\text{-}Y}$, $D_{b\text{-}G}$ in this example) via the reverse 3rd-masking model for Cases 2 and 3. Finally, the FDAs of RYG inks are obtained. As mentioned earlier, the $r_0$ is initially fixed. However, this value can occasionally achieve $(D_{r\text{-}R}, D_{g\text{-}Y}, D_{b\text{-}G}) > 1.0$ or $< 0.0$. In these cases, the $r_0$ will be optimized until a reasonable set of $(D_{r\text{-}R}, D_{g\text{-}Y}, D_{b\text{-}G})$ values can be obtained.

## TESTING MODELS' PERFORMANCE

The models derived were tested using all the characterization data sets which were used to derive these models. For testing the forward models, the 10 colorimetric measures were used, i.e. mean values of $|\Delta x|$, $|\Delta y|$, $\Delta u'v'$, $\Delta\%|Y|$, $|\Delta L|$, $|\Delta C|$, $|\Delta H|$, $\Delta E$ CIE $L^*a^*b^*$, $\Delta E$ CIE $L^*u^*v^*$, and $\Delta E$ CMC(1:1). For every color in each subset of 4-ink grouping, these 10 measures were calculated between the measured and predicted XYZ values. The mean measures from all the samples in each of the subsets of 4-ink grouping considered were used to represent the forward models predicted performance. For the comparison of the reverse models, the XYZ tristimulus values were first computed using predicted FDAs of four primaries via the forward model previously derived, and then the 10 mean measures mentioned above would be calculated between these predicted and measured XYZ values, and were used to represent the reverse models predicted performance. For simplification, the procedures for showing the performance test will also use the colors in the subgamut of KRYG as examples.

### The Performance of the Third-Order Masking Model

The 2nd characterization model derived here employs the 3rd-order masking model (Eqn. 2). Thus the predictive and the reversibility performance between the forward and reverse masking models was also checked in this investigation. The forward model computes the XYZ from three primaries excluding key ink, and the reverse model calculates three primaries used from XYZ. The evaluation was carried out using 216 samples in the cube data set produced using no key ink. The procedures for testing the predictive performance are given below:

$$(FDA_R, FDA_Y, FDA_G)_{Observed} \rightarrow \boxed{\text{Forward model}} \rightarrow (XYZ)_{Predicted} \overset{\text{Compare}}{\longleftrightarrow} (XYZ)_{Measured}$$

The observed FDAs of RYG inks of 216 colors were computed using the forward 3rd-masking model to predict the XYZ values. The agreement between the predicted and measured XYZ values for the 216 cube colors in terms of 10 colorimetric measures. (as mentioned earlier) represents the 3rd-order masking model reversibility performance. The results are given in Table 2. All measures for a perfect agreement, should equal zero for both the predictive and reversibility performance tests. The performance was considered to be very satisfactory. The mean CMC $\Delta E$ value of 1.52, 0.79, 1.21, 0.81, 0.75 and 1.67 were for the subgamuts of BKMC, RKYM, GKYC, KBMR, KGCB, and KRYG respectively.

Table 2. Summary of the 3rd-order masking equation's performance using the cube data set in each subset of 4-ink grouping

| 3rd-order masking model | | | | | | | | | | |
|---|---|---|---|---|---|---|---|---|---|---|
| Subgamut | \|△x\| | \|△y\| | △u'v' | %△\|Y\| | \|△L\| | \|△C\| | \|△H\| | △E L*a*b* | △E L*u*v* | △E CMC(1:1) |
| BKMC | 0.0044 | 0.0023 | 0.0045 | 3.70 | 0.76 | 0.75 | 0.81 | 1.91 | 2.65 | 1.52 |
| RKYM | 0.0017 | 0.0017 | 0.0016 | 1.68 | 0.35 | 0.35 | 0.45 | 0.97 | 1.14 | 0.79 |
| GKYC | 0.0030 | 0.0033 | 0.0025 | 2.52 | 0.52 | 0.57 | 0.71 | 1.55 | 1.84 | 1.21 |
| KBMR | 0.0028 | 0.0024 | 0.0033 | 1.66 | 0.34 | 0.38 | 0.48 | 1.34 | 1.83 | 0.81 |
| KGCB | 0.0010 | 0.0021 | 0.0020 | 1.91 | 0.39 | 0.26 | 0.46 | 1.08 | 1.17 | 0.75 |
| KRYG | 0.0052 | 0.0039 | 0.0037 | 2.82 | 0.58 | 0.78 | 1.10 | 2.52 | 2.95 | 1.67 |

## The Performance of the Forward Models

This test was conducted to investigate the predictive performance of the two forward models derived. The test procedures can be summarized as below:

$$(FDA_K, FDA_R, FDA_Y, FDA_G)_{Observed} \rightarrow \boxed{\text{Forward model}} \rightarrow (XYZ)_{Predicted} \overset{\text{Compare}}{\longleftrightarrow} (XYZ)_{Measured}$$

The observed FDAs of 4 primary inks of each color in the characterization data sets were input values to predict the XYZ values via each of two forward models. The predictive performance for each model was investigated by comparing the XYZ values between those predicted and measured, using the printing characterization data sets. The results are summarized in Table 3.

Table 3. Summary of the forward models' predictive performance

| 2nd model | | | | | | | | | | |
|---|---|---|---|---|---|---|---|---|---|---|
| Subgamut | \|△x\| | \|△y\| | △u'v' | %△\|Y\| | \|△L\| | \|△C\| | \|△H\| | △E L*a*b* | △E L*u*v* | △E CMC(1:1) |
| BKMC | 0.0044 | 0.0037 | 0.0053 | 4.25 | 0.84 | 0.68 | 0.80 | 1.98 | 2.43 | 1.54 |
| RKYM | 0.0028 | 0.0021 | 0.0026 | 2.58 | 0.52 | 0.48 | 0.66 | 1.46 | 1.88 | 1.10 |
| GKYC | 0.0030 | 0.0048 | 0.0030 | 2.85 | 0.57 | 0.70 | 0.64 | 1.87 | 1.99 | 1.26 |
| KBMR | 0.0051 | 0.0031 | 0.0049 | 3.92 | 0.76 | 0.60 | 0.86 | 1.84 | 2.50 | 1.48 |
| KGCB | 0.0021 | 0.0031 | 0.0029 | 3.32 | 0.66 | 0.50 | 0.63 | 1.42 | 1.56 | 1.19 |
| KRYG | 0.0052 | 0.0041 | 0.0043 | 3.86 | 0.77 | 0.91 | 1.21 | 2.31 | 2.79 | 1.95 |
| Cellular Neugebauer model | | | | | | | | | | |
| Subgamut | \|△x\| | \|△y\| | △u'v' | %△\|Y\| | \|△L\| | \|△C\| | \|△H\| | △E L*a*b* | △E L*u*v* | △E CMC(1:1) |
| BKMC | 0.0156 | 0.0071 | 0.0138 | 9.42 | 1.87 | 1.61 | 2.14 | 5.26 | 7.58 | 3.82 |
| RKYM | 0.0086 | 0.0044 | 0.0070 | 5.34 | 1.09 | 1.14 | 1.55 | 3.55 | 4.31 | 2.49 |
| GKYC | 0.0117 | 0.0065 | 0.0090 | 9.70 | 1.92 | 1.96 | 2.14 | 4.88 | 6.12 | 3.95 |
| KBMR | 0.0092 | 0.0199 | 0.0123 | 11.00 | 2.11 | 2.64 | 2.17 | 7.61 | 8.33 | 4.60 |
| KGCB | 0.0075 | 0.0102 | 0.0093 | 11.95 | 2.51 | 1.29 | 2.25 | 4.72 | 5.36 | 4.07 |
| KRYG | 0.0092 | 0.0062 | 0.0103 | 9.62 | 1.99 | 1.32 | 2.23 | 4.94 | 6.53 | 3.81 |

The 2nd model with mean CMC ΔE values of 1.54, 1.10, 1.26, 1.48, 1.19, and 1.95, for the subsets of BKMC, RKYM, GKYC, KBMR, KGCB, and KRYG respectively, performed much better than the Cellular Neugebauer model with mean CMC ΔE values of 3.82, 2.49, 3.95, 4.60, 4.07, and 3.81, for the subsets of BKMC, RKYM, GKYC, KBMR, KGCB, and KRYG respectively.

### The Performance of the Reverse Models

The two reverse models described earlier were also tested by examining the reversibility performance between the forward and reverse models using the characterization data sets. The forward model was used to calculate tristimulus values from the FDAs of 4 primary for each subset of 4-ink grouping, predicted using the corresponding reverse model. All measures should equal zero for perfect reversibility between the forward and reverse models. This test was carried out using the following procedures:

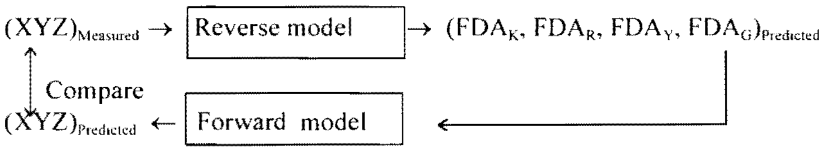


First, the reverse model (2nd or Cellular Neugebauer) was used to predict the FDAs of 4 primary inks (possibly applied using one of the 6 subsets of 4-ink grouping) from the measured XYZ tristimulus values for each characterization color in the supergamut of CMYKRGB. Second, the corresponding forward model was used to predict XYZ tristimulus values from these predicted FDAs of 4 primary inks.

Finally, the details of measures defining the reversibility performance were obtained by comparing between the predicted and the measured XYZ values. The results are shown in Table 4 for both of the 2nd and the Cellular Neugebauer models.

The frequency histograms were also produced to display the distribution of prediction errors using the CMC ΔE values. It gives a snapshot of the overall pattern of variations. The smaller the number of high ΔE values, with narrower distribution indicates a better performance such as that of the 2nd model. For a perfect agreement, all ΔE values should be located at the zero point. Figures 4 and 5 show the distribution of the mean CMC ΔE values for the 2nd and the Cellular Neugebauer models respectively.

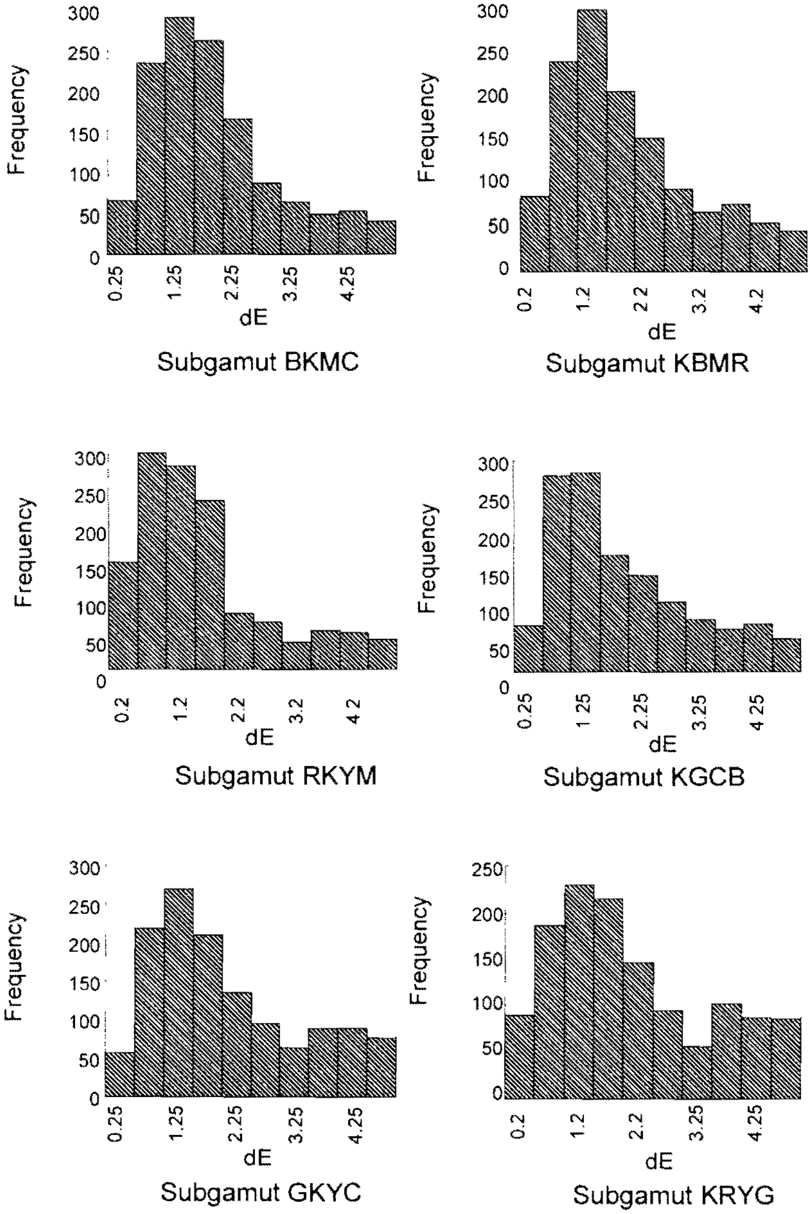


Figure 4. The ΔE(CMC) distributions for each of 6 subsets of 4-ink grouping using the reverse 2nd model.

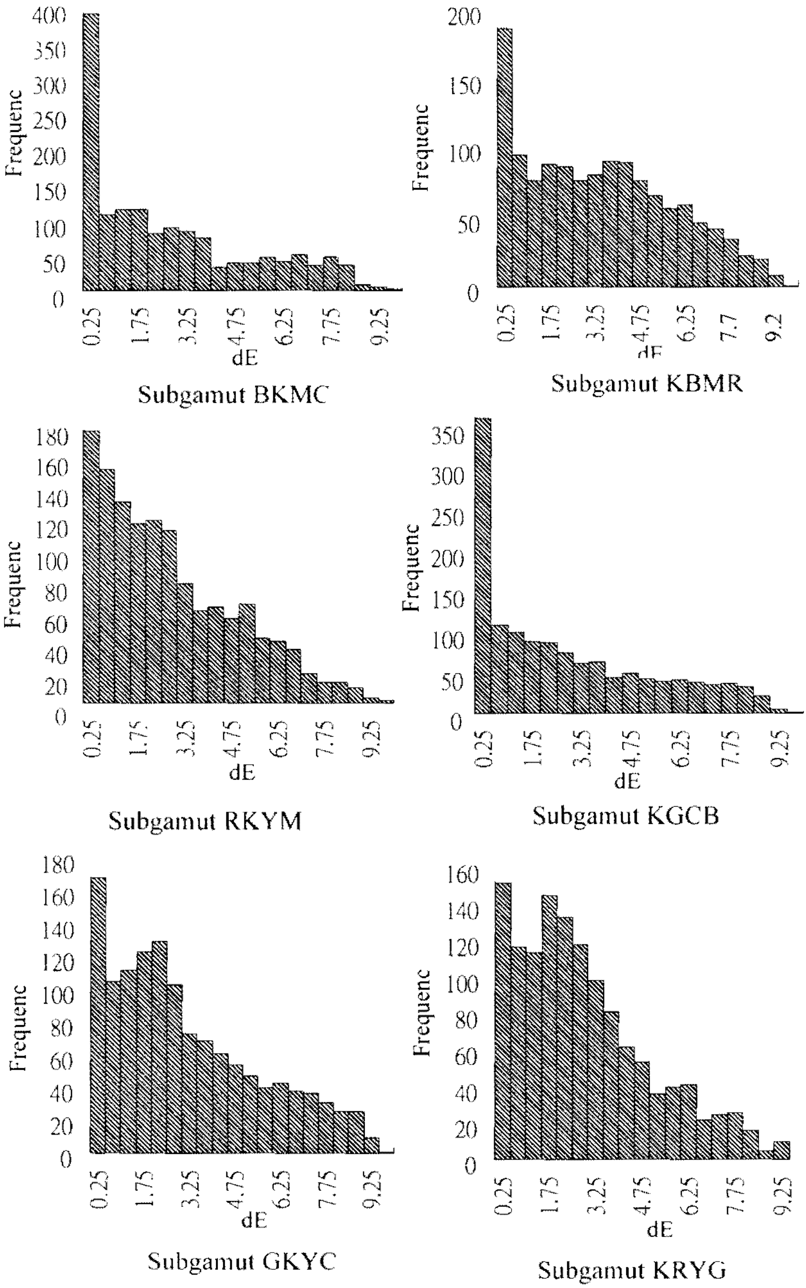


Figure 5. The ΔE(cmc) distributions for each of 6 subsets of 4-ink grouping predicted in the supergamut using the reverse cellular Neugebauer model.

Table 4. Summary of the reversibility performance for each of the reverse 2nd and Cellular Neugebauer model

| 2nd model | | | | | | | | | | |
|---|---|---|---|---|---|---|---|---|---|---|
| Subgamut | \|△x\| | \|△y\| | △u'v' | %△\|Y\| | \|△L\| | \|△C\| | \|△H\| | △E L*a*b* | △E L*u*v* | △E CMC(1.1) |
| BKMC | 0.0051 | 0.0044 | 0.0063 | 4.81 | 0.95 | 0.93 | 1.03 | 2.45 | 2.94 | 1.97 |
| RKYM | 0.0036 | 0.0038 | 0.0040 | 4.07 | 0.86 | 0.67 | 1.26 | 2.35 | 2.85 | 1.86 |
| GKYC | 0.0051 | 0.0068 | 0.0049 | 5.92 | 1.22 | 1.05 | 1.23 | 3.06 | 3.30 | 2.33 |
| KBMR | 0.0054 | 0.0046 | 0.0063 | 5.86 | 1.15 | 0.90 | 1.02 | 2.50 | 3.07 | 2.05 |
| KGCB | 0.0048 | 0.0045 | 0.0052 | 5.06 | 1.01 | 0.95 | 1.12 | 2.41 | 2.77 | 2.08 |
| KRYG | 0.0055 | 0.0053 | 0.0050 | 5.03 | 1.00 | 0.91 | 1.63 | 2.78 | 3.11 | 2.44 |
| Cellular Neugebauer Model | | | | | | | | | | |
| Subgamut | \|△x\| | \|△y\| | △u'v' | %△\|Y\| | \|△L\| | \|△C\| | \|△H\| | △E L*a*b* | △E L*u*v* | △E CMC(1.1) |
| BKMC | 0.0112 | 0.0134 | 0.0122 | 5.68 | 1.08 | 1.39 | 2.72 | 4.71 | 4.90 | 3.71 |
| RKYM | 0.0094 | 0.0055 | 0.0076 | 3.69 | 0.77 | 1.08 | 2.22 | 3.33 | 3.97 | 2.85 |
| GKYC | 0.0094 | 0.0060 | 0.0077 | 4.86 | 1.02 | 1.54 | 1.83 | 3.56 | 4.31 | 3.01 |
| KBMR | 0.0103 | 0.0102 | 0.0093 | 6.48 | 1.39 | 2.41 | 1.43 | 5.30 | 6.16 | 3.55 |
| KGCB | 0.0086 | 0.0097 | 0.0102 | 6.78 | 1.49 | 2.04 | 1.83 | 4.53 | 5.21 | 3.60 |
| KRYG | 0.0093 | 0.0111 | 0.0120 | 6.28 | 1.24 | 1.66 | 1.77 | 4.50 | 4.80 | 3.17 |

It is clearly shown that the 2nd model performed far better than the Cellular Neugebauer model for all the data sets. The variations of the mean CMC ΔE values for the all subsets using the 2nd model were much smaller than those for the Cellular Neugebauer model. The 2nd model predicted more accurate results than the Cellular Neugebauer model as seen from all the subsets used for characterization in table 4. The 2nd model gave reasonable predictions for all the 6 subsets. However, It was found that, to the neutral and near-neutral colors (for which (Dr, Dg, Db) are larger than (Dr, Dg, Db) of key ink in all the 6 subsets of 4-ink grouping) both of the 2nd and the Cellular Neugebauer gave the worst predictions amongst the samples studied. This suggests that a separate test target should be designed for the characterization of neutral and near-neutral colors. Also, two models performed worse for the colorful samples having high saturation and less gray contents than those not so colorful (i.e. with less saturation.) This indicates that the highly saturated data set provides a more critical test than those less saturated for the models derived.

## CONCLUSIONS

Two models were successfully derived to characterize the 7-ink printing process using FM screening. The following conclusions may be drawn:

Overall, the 2nd model performed better than the Cellular Neugebauer model. For the forward models' performance, the 2nd model performed better than the Cellular Neugebauer model. For the reversibility performance of the reverse models, the 2nd model always gave better performance than the Cellular Neugebauer model. The reversibility performance for the 2nd model was quite satisfactory.

However, a separate test target is required for individually characterizing neutral and near-neutral colors due to the results obtained showing that both of the 2nd and the Cellular Neugebauer models gave worse predictions to those neutral and near-neutral colors amongst all the data sets. Additionally, the highly colorful samples provide a very critical test of the performance for the models derived, since the results obtained showed that both of the characterization models gave less accurate predictions to the purer and more saturated samples compared to those of the samples having less chroma or more gray contents in all the data sets from the 6 subsets of 4-ink grouping.

## ACKNOWLEDGEMENTS

This research has been mainly financed by the Industrial Technology Research Institute, Taiwan,R.O.C., and also supported by Shen's Art Printing Co., Taiwan, R.O.C., for preparing samples and supplying the spectrophotometer for color measurement.

## REFERENCES

Clapper, F. R.
1961. "An empirical determination of half-tone colour-reproduction requirement", TAGA Proc., pp.31-41.

Clapper, F. R. and Yule, J. A. C.
1953. "The effect of multiple internal reflection on the densities on halftone-tone printing paper", J. Opt. Soc. Am., 43, pp.600-603.

Heuberger, K. J., Jing, Z. M. and Persiev, S.
1992. "Color transformations and lookup tables", TAGA/ISCC Proc., **2**, pp. 863-881.

Harold Boll
1993. "A color to colorant transformation for a seven ink process", SPIE ,vol.2170,pp.108-118.

Humbel V. et al.
1992. "The benefits of frequency modulation screening." EMPA/UGRA project no.89/2. St. Gallen 992.

Johnson, A. J., Luo M. R., Lo, M. C., Xin J. H. and Rhodes, P. A.
1995a "Aspects of colour management. Part I. Characterization of three-colour imaging devices", Color Res. Appl., 20.

Johnson, A. J., Luo M. R., Lo, M. C., Xin J. H. and Rhodes, P. A.
1995b "Aspects of colour management. Part II. Characterization of four-colour imaging devices and colour gamut compression", Color Res. Appl., 20.

Karl J. Heuberger, Zhon Mo Jing,Serdar Persiev
1992. "Color transformations and lookup tables", TAGA proceedings,vol 2,pp.863-882.

Lawson, C. L. and Hanson, R.
1974. "Solving Least Squares Problems", Englewood Cliffs, NJ: Prentice-Hall.

Lo, M. C.
1995. "The LLab model for quantifying colour appearance", doctoral thesis of Loughborough University.
Lo, M. C. and Luo, M. R.
1994. "Models for characterizing four-primary printing devices", Photo. Sci., 42, pp.94-96.
Luo, M .R.. Johnson, Xin, A., J. H., Rhodes, P.A. and Scrivener, S. A. R.,
1992. "Mathematical Models for Characterising Printing Devices", SID'92 Digest, Boston, May, pp.753-756.
Murray, A.
1936. "Monochrome reproduction in photoengraving", J. Franklin Inst., pp.721-744.
Neugebauer, H. E. J.
1937. "Die Theoretischen grundlagen des methrfarbendruckes", zeitshrift wissenschaften photograph, 36, pp.73-89.
Pobboravsky, I. and Pearson, M. L.
1972. "Computation of dot areas required to match a colorimetrically specified color using the modified Neugebauer equations, TAGA Proc., 65-77 (1972).
Rolleston, R. and Balasubramanian, R.
1993. "Accuracy of various types of Neugebauer model", IS&T and SID Colour Imaging Conference: Transforms & Transportability of color, pp.32-37.
Stearns, E. I.
1985. "Calculation of tristimulus values and weights with the revised CIE recommendations", Textile Color Col. Chemist and Colorist, 53, pp.162-168.
Stearns, E. I.
1975. "Weights for calculation of tristimulus values", Clemson University Review of Industrical Management and Textile Science, 14, pp.79-112.
Yule, J. A. C. and Colt, R. S.
1951 "Colorimetric investigations in multi-colour printing", TAGA Proc., pp.77-82.
Yule, J. A. C.
1967. "Principle of Colour Reproduction", John Wiley & Sons, p.282.
Yule, J. A. C.
1938 "The theory of subtractive colour photography"; I. The conditions for perfect colour rendering, J. Opt. Soc. Am., 28,pp.419-430.
Yule, J. A. C. and Nielsen, W. J.
1951 "The penetration of light into paper and its effect on halftone reproduction", TAGA Proc., pp.65-76.